Details of the Potential Energy Surface for the Reaction Y + H₂CCO: A Crossed-Beams Study

Jonathan J. Schroden, Maurice Teo, and H. Floyd Davis*

Department of Chemistry and Chemical Biology, Cornell University, Ithaca, New York 14853

Received: June 19, 2002; In Final Form: September 5, 2002

The reaction of ground-state Y ($a\ ^2D$) atoms with ketene (H_2CCO) was studied at two collision energies, 22.7 and 10.4 kcal/mol. At both collision energies, four competing processes were observed corresponding to formation of YCH_2, YCCO, YCHCO (with elimination of CO, H_2, and H, respectively), and nonreactive scattering. The endoergicity of the YCHCO + H product channel was 10.5 ± 2.0 kcal/mol, leading to $D_0(Y-CHCO) = 93.4 ± 2.0$ kcal/mol. Product branching ratios measured at both collision energies show formation of YCH_2 + CO to be dominant. The trend in branching ratios as a function of collision energy, combined with center-of-mass distributions obtained through fits to the experimental data and analogies to the Y + H_2CO system, allows a qualitative description of relevant features of the Y + H_2CCO potential energy surface.

Introduction

Over the past several years, crossed molecular beam experiments have been used to study insertion reactions of metal atoms into carbon–hydrogen and carbon–carbon bonds.[1–11] These reactions are interesting from a fundamental point of view, since they allow the effects of electronic structure on reactivity to be observed directly, without complications due to solvent and ligand effects. They are also simple models for catalytic processes of great importance industrially. The crossed molecular beam technique is a particularly powerful probe of reaction dynamics, and its application to these types of reactions has been quite successful. Recently, Weisshaar and co-workers have studied the dynamics of reactions of Co^+ ($^3F_4$) and Ni^+ ($^2D_{5/2}$) with several alkanes[6–10] and also with acetone.[11] The results of these studies, in conjunction with ab initio calculations and statistical modeling,[12] have shown the importance of multicentered transition states (MCTS) along the reaction pathway, illustrating that the preferred mechanism for reaction is often concerted and not stepwise, as was thought earlier.[6–12]

In reactions of neutral, ground-state Y (^2D), Zr (^3F), and Nb (^6D) and excited-state Mo* ($^5S_2$) with small hydrocarbons such as methane,[2,4] ethane,[1] ethylene,[4] and acetylene,[5] only products from C–H insertion were observed. However, reactions of larger hydrocarbons such as cyclopropane and propene yielded products from both C–H and C–C insertion.[13] The branching ratios for competing processes have provided insight into the potential energy surfaces. We have also studied neutral transition-metal atom reactions with carbonyl-containing molecules. The reaction of yttrium with formaldehyde (H_2CO) led to two products, YH_2 and YCO, at all collision energies studied and a third product channel, YCHO, at high collision energies (31 kcal/mol). The YH_2 + CO product channel was dominant due to the greater exothermicity of YH_2 formation and a proposed potential energy barrier for YCO formation.[3] A recent ab initio study has confirmed the existence of a barrier to H_2 elimination.[14] These calculations, combined with RRKM theory, allowed us to

quantitatively reproduce the measured branching ratios between YCO and YCHO formation with only slight adjustments to the ab initio potential energy surface.[15]

We have also investigated reactions of yttrium with the methylated analogues of formaldehyde, namely, acetaldehyde and acetone.[16] Products from elimination of CO, H_2, and H were observed at high collision energies. Translational energy distributions for CO elimination, which was the dominant product channel, indicated that a significant fraction of the available energy was channeled into product translation due to the existence of a substantial potential energy barrier for formation of a (R)(R′)YCO (R, R′ = H, CH_3) intermediate and incomplete energy randomization prior to dissociation.

Ketene is unusual because of the presence of adjacent C=C and C=O bonds, as well as a weak C=C bond. Its reactions with metal atoms are interesting because they lead to competing product channels involving production of prototype metallic species such as YCH_2 and YCCO, by elimination of important ligands such as CO and H_2, respectively.

Experimental Section

The experiments were conducted with a rotatable source crossed molecular beam apparatus.[17] The 532-nm output of a Nd:YAG laser (Continuum Surelite) was focused onto a 0.25-in.-diameter yttrium rod (Alfa Aesar, 99% purity). The ablated yttrium atoms were subsequently entrained in a supersonic inert gas pulse[17,18] (He or Ne, 5 psig), forming the metal beam which was then skimmed, collimated, and chopped by a slotted chopper wheel spun at 210 Hz. Ketene was prepared by pyrolysis of acetic anhydride[19] (Aldrich, 99% purity), trapped at 77 K, and subsequently purified by trap-to-trap distillations using dry ice-acetone and liquid nitrogen baths. The ketene beam was generated by passing an inert carrier gas (He, 5 psig) through a bubbler containing pure liquid ketene held at −78 °C. The resulting mixture was sent to a second pulsed valve. The ketene beam was also skimmed before crossing the yttrium beam at 90°. Electron impact ionization was used to measure the velocity distributions of both beams, using the time-of-flight (TOF) method.[17] Parameters relevant to the beam profiles are given

---

* To whom correspondence should be addressed. E-mail: hfd1@cornell.edu.
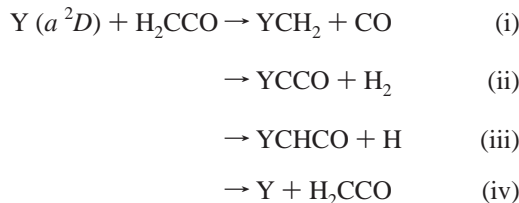
TABLE 1: Experimental Conditions for Y + H$_2$CCO Studies

$<E_{coll}>$, kcal/mol	yttrium carrier gas	H$_2$CCO conditions	Y beam parameters		H$_2$CCO beam parameters	
			v_{pk}, m/s	fwhm	v_{pk}, m/s	fwhm
22.7	He	78 °C in He	2240	292	1250	114
10.4	Ne	78 °C in He	1220	134	1250	114

in Table 1. The yttrium beam has been shown to consist only of two spin−orbit states of the ground electronic state, Y(a $^2D_{3/2}$) and Y(a $^2D_{5/2}$).[5]

Metallic products from reactive and nonreactive collisions traveled 24.1 cm to the detector, where they were ionized at 157 nm using an F$_2$ excimer laser (LPX220i).[17] By scanning the delay time of the excimer trigger with respect to a time zero for reaction, product TOF spectra were obtained. Integration of these spectra at different angles yielded the lab angular distribution, $N(\Theta)$. By use of a forward-convolution program with instrumental and experimental parameter inputs (aperture sizes, flight distances, beam velocities, etc.), along with two center-of-mass (CM) input functions (the translational energy release distribution, $P(E)$, and the CM angular distribution, $T(\theta)$), TOF spectra and lab angular distributions were calculated and compared with experimental data. The two CM functions were iteratively adjusted until calculated angular distributions and TOF spectra matched those from experiment.

Results

E_{coll} = **22.7 kcal/mol.** Collisions of Y(a ^2D) atoms with ketene (H$_2$CCO) at E_{coll} = 22.7 kcal/mol resulted in four processes:

$$Y(a\,^2D) + H_2CCO \rightarrow YCH_2 + CO \quad\quad (i)$$
$$\rightarrow YCCO + H_2 \quad\quad (ii)$$
$$\rightarrow YCHCO + H \quad\quad (iii)$$
$$\rightarrow Y + H_2CCO \quad\quad (iv)$$

The TOF spectra for YCCO and YCHCO (recorded at m/e 129 and 130, respectively) are shown in Figure 1, while TOFs for YCH$_2$ (recorded at m/e 103) are shown in Figure 2. Because of the small mass of H and H$_2$, YCHCO and YCCO are confined to a narrower range of laboratory angles than YCH$_2$, which recoils from CO (Figure 3). Although the TOF spectra for YCHCO and YCCO look similar at this collision energy, Figure 3 clearly shows that the YCCO lab angular distribution is wider than that for YCHCO, indicating that YCCO formation is a distinct product channel and not a result of dissociative ionization of YCHCO. The solid-line fits shown in Figures 1−3 for YCH$_2$ and YCCO were generated using the CM distributions shown in Figure 4. The CM distributions used to generate the fits for YCHCO in Figures 1 and 3 are similar in shape to those for YCCO and are not shown. The translational energy distribution, $P(E)$, for YCH$_2$ peaks quite far from the zero of kinetic energy, with $\langle P(E) \rangle$ = 13.9 kcal/mol. The $P(E)$ for YCCO peaks slightly closer to the zero of energy, with $\langle P(E) \rangle$ = 12.4 kcal/mol, while that for YCHCO peaks significantly closer to zero, with $\langle P(E) \rangle$ = 8.7 kcal/mol, respectively. The CM angular distributions for YCCO and YCHCO are isotropic (i.e., $T(\theta = 0°)/T(\theta = 90°) = 1$), as is common for reactions eliminating light counterfragments based on angular momentum considerations.[20] The CM angular distribution for YCH$_2$ exhibits peaks in both the forward ($\theta = 0°$) and backward ($\theta = 180°$)
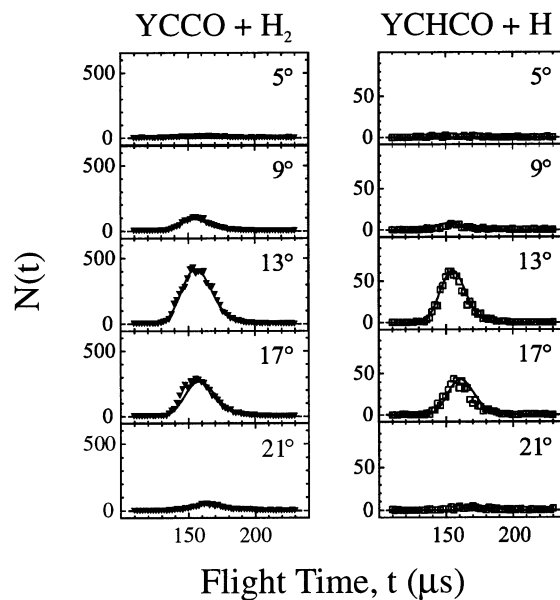

Figure 1. Time-of-flight (TOF) spectra for YCCO and YCHCO (closed triangles and open squares, respectively) for indicated lab angles at E_{coll} = 22.7 kcal/mol. Solid-line fits generated by using CM distributions shown in Figure 4.
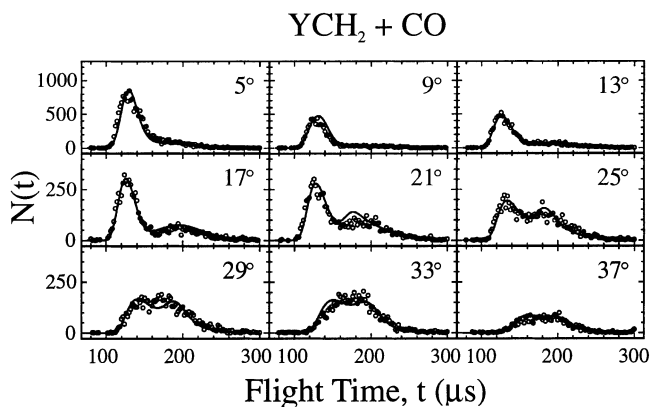

Figure 2. TOF spectra for YCH$_2$ (open circles) for indicated lab angles at E_{coll} = 22.7 kcal/mol. Solid-line fits generated by using CM distributions shown in Figure 4.

directions. Interestingly, the $T(\theta)$ for YCH$_2$ is not symmetric about $\theta = 90°$, contrasting the $T(\theta)$s for all other products from Y, Zr, Nb, and Mo reactions observed previously in our laboratory.

The TOF spectra for nonreactively scattered yttrium atoms (recorded at m/e 89) are shown in Figure 5. At small lab angles, only one peak is seen in the TOF, while at larger angles a second peak becomes discernible. The corresponding lab angular distribution is shown in Figure 6. The fits shown in Figures 5 and 6 are the sum of those for two processes generated by using the CM distributions shown in Figure 7. One corresponds to direct inelastic scattering (dotted lines) and the other to decay of a Y−H$_2$CCO complex (dash−dot lines). The P(E) for direct inelastic scattering looks similar to the collision energy distribution (solid line), but shifted to lower translational energies, with $\langle P(E) \rangle$ = 14.9 kcal/mol. The $T(\theta)$ for this process is strongly peaked in the forward direction, as expected for a process without complex formation. The $P(E)$ for decay of Y−H$_2$CCO complexes is shifted to much lower translational energies, with $\langle P(E) \rangle$ = 8.9 kcal/mol, indicating that a larger average fraction of the initial collision energy is deposited into internal degrees of freedom of H$_2$CCO (60.8% versus 34.4% for direct inelastic
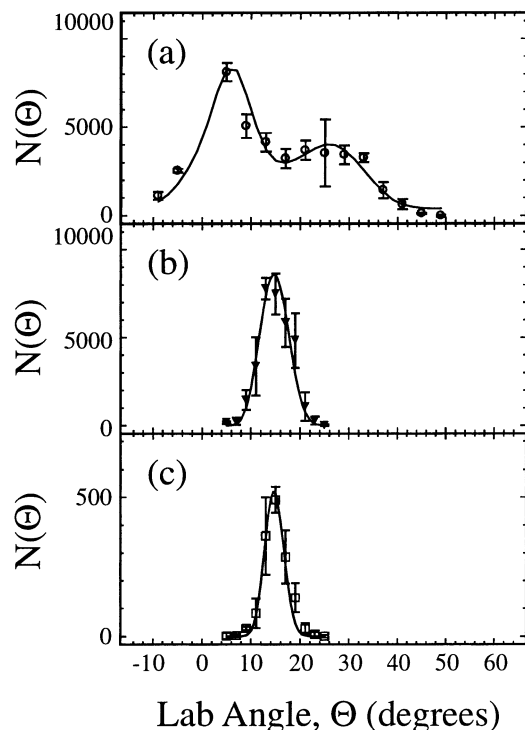
Details of the Potential Energy Surface

J. Phys. Chem. A, Vol. 106, No. 48, 2002 **11697**

Figure 3. Lab angular distributions at $E_{coll} = 22.7$ kcal/mol for (a) YCH$_2$, (b) YCCO, and (c) YCHCO. Each angular distribution corresponds to one scan at each laboratory angle. Solid-line fits generated by using CM distributions shown in Figure 4.
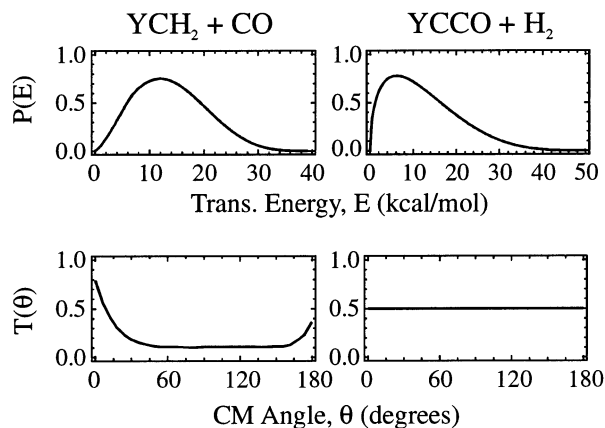

Figure 4. CM distributions used to fit experimental data for YCH$_2$ and YCCO at $E_{coll} = 22.7$ kcal/mol. Top: Translational energy distributions, P(E). Bottom: CM angular distributions, $T(\theta)$.

scattering). The $T(\theta)$ for complex decay is forward−backward symmetric and peaks near the poles ($\theta = 0°$ and $\theta = 180°$), as expected from angular momentum considerations.[20]

To accurately determine branching ratios for competing channels, it was necessary to consider the photoionization cross sections, fragmentation patterns, and Jacobian factors for each reaction. In this study, the product fragmentation patterns and Jacobian factors were explicitly included in the analysis. The photoionization cross sections were assumed to be identical for each product, which we justify from results in an earlier study.[13] The branching ratios were $\phi_{YCH_2}:\phi_{YCCO}:\phi_{YCHCO} = 8.82:1.0:0.43$, indicating that YCH$_2$ formation was by far the dominant process at $E_{coll} = 22.7$ kcal/mol.

$E_{coll} = $ **10.4 kcal/mol.** The reaction Y + H$_2$CCO was also studied at $E_{coll} = 10.4$ kcal/mol. Although all four product channels were observed, the YCHCO signal was extremely weak. The TOF spectra for YCH$_2$ and YCCO are very similar
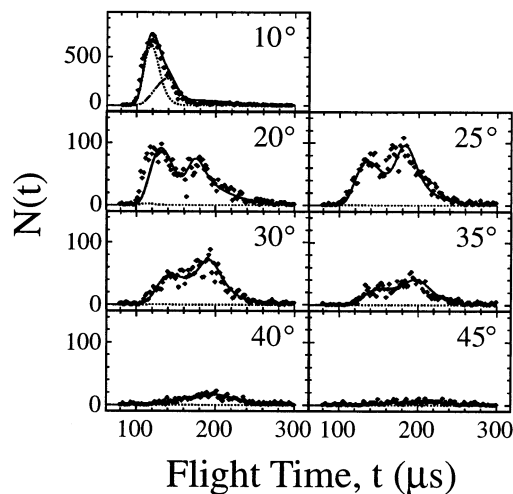

Figure 5. TOF spectra for nonreactively scattered yttrium atoms (open diamonds) for indicated lab angles at $E_{coll} = 22.7$ kcal/mol. Solid-line fits generated by using CM distributions shown in Figure 7. Dotted line indicates contribution from inelastic scattering, while dash−dot line indicates contribution from π-complex decay (overlapped by the solid line at larger angles).

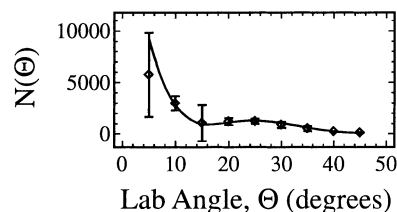**Figure 6.** Lab angular distribution for nonreactively scattered yttrium atoms at $E_{coll} = 22.7$ kcal/mol (open diamonds), corresponding to two scans at each laboratory angle. Solid-line fit generated by using CM distributions shown in Figure 7.
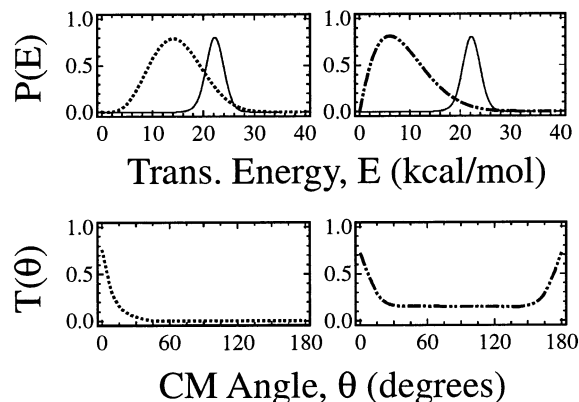

Figure 7. CM distributions used to fit nonreactive scattering data at $E_{coll} = 22.7$ kcal/mol. Solid lines in the P(E) correspond to the collision energy distribution, dotted lines indicate distributions for inelastic scattering, and dash−dot lines indicate distributions for π-complex decay.

to those obtained at the higher collision energy and are not shown. The lab angular distributions for YCH$_2$ and YCCO are shown in Figure 8. The CM distributions used to fit the data are similar to those shown in Figure 4 and are not shown. Based on the fits to the experimental data, the branching ratios at this collision energy were $\phi_{YCH2}:\phi_{YCCO}:\phi_{YCHCO} = 35.2:1.0:0.1$.

Discussion

Although no electronic structure calculations have been carried out for the title reaction, analogies with Y + H$_2$CO,
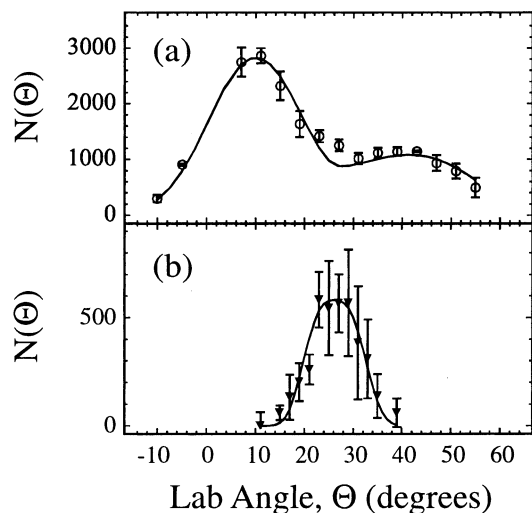
Figure 8. Lab angular distributions at $E_{coll} = 10.4$ kcal/mol for (a) YCH_2 and (b) YCCO. Each angular distribution corresponds to one scan at each laboratory angle.
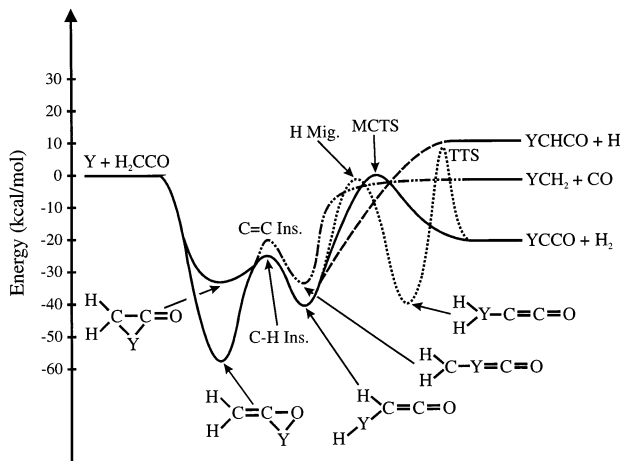

Figure 9. Schematic potential energy surface diagram for Y + H_2CCO drawn by analogy to ab initio calculations on Y + H_2CO.[14] Following initial π-complex formation, the solid line indicates a concerted pathway leading to YCCO, the dotted line indicates a stepwise pathway leading to YCCO, the dash−dot line indicates a pathway to YCH_2, and the dashed line indicates a pathway to YCHCO.

which has been studied theoretically, can be used to gain insight into the Y + H_2CCO reaction. A schematic potential energy diagram for Y + H_2CCO is shown in Figure 9. The energetics of intermediates in this figure have been estimated by comparison to the Y + H_2CO potential energy surface.[14] The energetics of the YCH_2 and YCCO product asymptotes have been estimated by using available thermodynamic values,[21−23] with the Y−CCO bond strength taken to be similar to that of Y−CCH_2.[24] The endoergicity of YCHCO formation was explicitly measured as described below.

The Y + H_2CCO reaction, like many reactions involving molecules containing π−bonds, is initiated via complex formation between the yttrium atom and a multiple bond. Evidence for complex formation can be seen in the nonreactive scattering data, as discussed above. Ketene presents a case in which there exist two possible binding sites: a C=C bond and a C=O bond. Presumably yttrium could bind to either or both sites. Recent ab initio calculations for Y + C_2H_4 have placed the depth of the Y−C_2H_4 π-complex well at about 30 kcal/mol below reactants,[25] whereas Y−H_2CO has been calculated to lie 57 kcal/mol below.[14] While this is a large difference in binding energies,

it is plausible that both complexes can be formed. Following formation of a Y−H_2CCO complex, yttrium can either insert into the C=C bond to form H_2CYCO or insert into a C−H bond to form HYCHCO. Insertion into the C=C bond leads to an H_2CYCO intermediate which can decay to YCH_2 and CO (dash−dot line in Figure 9). The steps after C−H insertion involve either elimination of an H atom to form YCHCO (dashed line in Figure 9), or migration of H followed by formation of YCCO (with elimination of H_2). In early investigations of H_2 elimination from hydrocarbons by yttrium atoms,[1,3,5,26] mechanisms were proposed involving β-hydrogen migration to Y, forming intermediates that subsequently decayed over a tight transition state (TTS) to eliminate H_2. Such mechanisms were proposed to explain the large product translational energy releases and were rationalized in terms of electronic structure.[5] However, recent ab initio calculations on H_2 elimination from C_2H_4[25] and H_2CO[14] by yttrium have shown that the mechanisms with the lowest potential energy barriers involve β-hydrogen migration over multicentered transition states (MCTS), leading to concerted H_2 elimination without formation of a dihydride intermediate.[14,25] Since this MCTS lies above the products, it is a true exit-channel barrier, leading to the large translational energy release for H_2 elimination. Figure 9 shows both the stepwise and concerted mechanisms (dotted and solid lines, respectively) for Y + $H_2CCO \rightarrow$ YCCO + H_2. On the basis of the similar structures of ketene and formaldehyde, and the similar $P(E)$ for H_2 elimination, it seems likely that this channel also involves a concerted mechanism.

For a molecule such as ethylene, one would expect insertion into the C=C bond to encounter a significantly larger barrier than that for insertion into a C−H bond for several reasons. First, the C=C bond of ethylene is stronger than a C−H bond by about 60 kcal/mol.[27] Second, it should be easier to insert into a C−H bond than a C=C bond due to the spherical nature of the H 1s orbital, which allows for multi-center bonding, thereby reducing the energy at the transition state. This contrasts the very directional sp[2]-hybridized C=C bond.[26,28,29] Ketene presents an interesting exception, however, because the C=C bond is 30 kcal/mol *weaker* than a typical C−H bond.[22,30] Consequently, the C=C and C−H insertion barrier heights for ketene could be comparable.

The measured branching ratio ϕ_{YCH_2}:ϕ_{YCCO} can be used to make further statements about the potential energy barrier heights. Formation of YCH_2 + CO was more favorable than YCCO + H_2 by a factor of 8.82 at the high collision energy and by a factor of 35.2 at the lower collision energy. The fact that YCH_2 formation becomes more dominant at lower collision energies suggests that the C=C insertion barrier, which should be the largest barrier leading to formation of YCH_2, must be lower than the MCTS for H_2 elimination shown in Figure 9. The shape of the CM angular distribution for YCH_2 is not symmetric about $\theta = 90°$, indicating that a substantial fraction of reactions proceed through short-lived intermediates having lifetimes less than one rotational period. This implies that any potential energy well on the surface leading to YCH_2 products must be shallow. This reaction almost certainly involves formation of an initial π-complex with the C=C bond, followed by insertion. The large translational energy release for YCH_2 indicates that complexes that surmount the C=C insertion barrier dissociate before the available energy is fully randomized. This is consistent with a shallow well for the H_2CYCO intermediate and is similar to the dynamics of CO elimination in reactions of yttrium with H_2CO, CH_3CHO, and CH_3COCH_3.[16]

Details of the Potential Energy Surface

J. Phys. Chem. A, Vol. 106, No. 48, 2002 **11699**

The fact that the YCHCO signal was weak at E_{coll} = 10.4 kcal/mol suggested that this collision energy was near the thermodynamic threshold. Therefore, additional data were taken at a slightly higher collision energy of 11.2 kcal/mol. To fit both sets of data, it was necessary to include a reaction threshold energy of 10.5 ± 0.5 kcal/mol. This corresponds to a steplike cutoff in the collision energy distribution, such that reactants with total energy less than this amount are unable to form products. In the case of Y + H_2CO, ab initio calculations found no potential energy barriers in excess of the reaction endoergicity for formation of YCHO + H products.[14] Given the similarity of Y + H_2CO to Y + H_2CCO, we expect that no potential energy barrier exists in excess of the endoergicity for YCHCO + H production. Therefore, the measured threshold corresponds to the endoergicity. Since YCHCO may result from reaction of the Y ($a\,^2D_{3/2}$) ground state or the Y ($a\,^2D_{5/2}$) spin−orbit excited-state lying 1.5 kcal/mol higher in energy, we conclude that the endoergicity of the Y + $H_2CCO \rightarrow$ YCHCO + H reaction is 10.5 ± 2.0 kcal/mol. Based on the literature value for the C−H bond strength of ketene,[27,30] we find that D_0(Y−CHCO) = 93.4 $\pm$ 2.0 kcal/mol.

Conclusion

The reaction of ground-state yttrium atoms with ketene was studied at two collision energies. At both collision energies, we observed formation of YCH_2, YCCO, YCHCO (with elimination of CO, H_2, and H, respectively), and nonreactive scattering. Measured product branching ratios indicate that at both collision energies, formation of YCH_2 was the dominant reactive channel. The trend of the branching ratios as a function of collision energy suggests that the C=C insertion barrier lies below the multicentered transition state (MCTS) for H_2 elimination. Also, thermodynamic arguments suggest the height of the C=C insertion barrier should be similar to that for C−H insertion. The translational energy distributions used to fit the experimental data indicated that a large fraction of the available energy appeared as translation of YCH_2 and YCCO. The CM angular distributions for YCCO and YCHCO were forward−backward symmetric, indicating the existence of at least one long-lived intermediate. The CM angular distribution for YCH_2 was not forward−backward symmetric, suggesting that the H_2CYCO intermediate is short-lived. Formation of YCCO products most likely occurs via a concerted mechanism involving a MCTS lying above the product asymptote, as in other reactions involving yttrium leading to H_2 elimination. Formation of YCHCO + H most likely involves no reverse barrier, allowing the measured energetic threshold of 10.5 ± 2.0 kcal/mol to be equated to the reaction endoergicity.

References and Notes

(1) Stauffer, H. U.; Hinrichs, R. Z.; Schroden, J. J.; Davis, H. F. *J. Phys. Chem. A* **2000**, *104*, 1107.

(2) Hinrichs, R. Z.; Willis, P. A.; Stauffer, H. U.; Schroden, J. J.; Davis, H. F. *J. Chem. Phys.* **2000**, *112*, 4634.

(3) Stauffer, H. U.; Hinrichs, R. Z.; Schroden, J. J.; Davis, H. F. *J. Chem. Phys.* **1999**, *111*, 10758.

(4) Willis, P. A.; Stauffer, H. U.; Hinrichs, R. Z.; Davis, H. F. *J. Phys. Chem. A* **1999**, *103*, 3706.

(5) Stauffer, H. U.; Hinrichs, R. Z.; Willis, P. A.; Davis, H. F. *J. Chem. Phys.* **1999**, *111*, 4101.

(6) Yi, S. S.; Reichert, E. L.; Holthausen, M. C.; Koch, W.; Weisshaar, J. C. *Chem. Eur. J.* **2000**, *12*, 2232.

(7) Reichert, E. L.; Yi, S. S.; Weisshaar, J. C. *Int. J. Mass. Spectrom.* **2000**, *195/196*, 55.

(8) Blomberg, M.; Yi, S. S.; Noll, R. J.; Weisshaar, J. C. *J. Phys. Chem. A* **1999**, *103*, 7254.

(9) Noll, R. J.; Yi, S. S.; Weisshaar, J. C. *J. Phys. Chem. A* **1998**, *102*, 386.

(10) Noll, R. J.; Weisshaar, J. C. *J. Am. Chem. Soc.* **1994,** *116*, 10288.

(11) Yi, S. S.; Reichert, E. L.; Weisshaar, J. C. *Int. J. Mass. Spectrom.* **1999**, *185/186/187*, 837.

(12) Yi, S. S.; Blomberg, M. R. A.; Siegbahn, P. E. M.; Weisshaar, J. C. *J. Phys. Chem. A* **1998**, *102*, 395.

(13) Hinrichs, R. Z.; Schroden, J. J.; Davis, H. F., to be published.

(14) Bayse, C. A. *J. Phys. Chem. A* **2002**, *106*, 4226.

(15) Schroden, J. J.; Davis, H. F.; Bayse, C. A., to be published.

(16) Schroden, J. J.; Teo, M.; Davis, H. F., submitted to *J. Chem. Phys.*

(17) Willis, P. A.; Stauffer, H. U.; Hinrichs, R. Z.; Davis, H. F. *Rev. Sci. Instrum.* **1999**, *70*, 2606.

(18) Powers, D. E.; Hansen, S. G.; Geusic, M. E.; Puiu, A. C.; Hopkins, J. B.; Dietz, T. G.; Duncan, M. A.; Langridge-Smith, P. R. R.; Smalley, R. E. *J. Phys. Chem.* **1982**, *86*, 2556.

(19) (a) Vogt, J.; Williamson, A. D.; Beauchamp, J. L. *J. Am. Chem. Soc.* **1978**, *100*, 3478. (b) Andreades, S.; Carlson, H. D. *Org. Synth.* **1965**, *45*, 50.

(20) (a) Miller, W. B.; Safron, S. A.; Herschbach, D. R. *Discuss. Faraday Soc.* **1967**, *44*, 108. (b) Miller, W. B.; Safron, S. A.; Herschbach, D. R. *J. Chem. Phys.* **1972**, *56*, 3581.

(21) Thermodynamics Research Center, NIST Boulder Laboratories, M. Frenkel director. Thermodynamics Source Database. In *NIST Chemistry WebBook, NIST Standard Reference Database Number 69;* Linstrom, P. J., Mallard, W. G., Eds.; National Institute of Standards and Technology: Gaithersburg MD, July 2001; p 20 899 (http://webbook.nist.gov).

(22) Ruscic, B.; Litorja, M.; Asher, R. L. *J. Phys. Chem. A* **1999**, *103*, 8625.

(23) Siegbahn, P. E. M. *Chem. Phys. Lett.* **1993**, *201*, 15.

(24) Glendening, E. D.; Strange, M. L. *J. Phys. Chem. A* **2002**, *106*, 7338.

(25) Porembski, M.; Weisshaar, J. C. *J. Phys. Chem. A* **2001**, *105*, 6655.

(26) Carroll, J. J.; Haug, K. L.; Weisshaar, J. C.; Blomberg, M. R. A.; Siegbahn, P. E. M.; Svensson, M. *J. Phys. Chem.* **1995**, *99*, 13955.

(27) Berkowitz, J.; Ellison, G. B.; Gutman, D. *J. Phys. Chem.* **1994**, *98*, 2744.

(28) Low, J. J.; Goddard, W. A., III *J. Am. Chem. Soc.* **1984**, *106*, 8321.

(29) Blomberg, M. R. A.; Siegbahn, P. E. M.; Nagashima, U.; Wennerberg, J. *J. Am. Chem. Soc.* **1991**, *113*, 424.

(30) Bauschlicher, C. W., Jr.; Langhoff, S. R. *Chem. Phys. Lett.* **1991**, *177*, 133.